Available online at www.sciencedirect.com
SCIENCE DIRECT®

Journal of the European Ceramic Society 23 (2003) 2193–2202
www.elsevier.com/locate/jeurceramsoc

Microstructure and properties of $CaO–ZrO_2–SiO_2$ glass–ceramics prepared by sintering

K.J. Hong, J.M. Kim, H.S. Kim*

Department of Materials Science and Metallurgical Engineering, Sunchon National University, 540-742, South Korea

Received 8 July 2002; received in revised form 14 January 2003; accepted 24 January 2003

Abstract

For the development of a new wear resistant and chemically stable glass-ceramic glaze, the $CaO–ZrO_2–SiO_2$ system was studied. Compositions consisting of CaO, ZrO_2, and SiO_2 were used for frit, which formed a glass-ceramic under a single stage heat treatment in electric furnace. In the sintered glass-ceramic, wollastonite ($CaSiO_3$) and calcium zirconium silicate ($Ca_2ZrSi_4O_{12}$) were crystalline phases composed of surface and internal crystals in the microstructure. The internal crystal formed with nuclei having a composition of $Ca_{1.2}Si_{4.3}Zr_{0.2}O_8$. The $CaO–ZrO_2–SiO_2$ system showed good properties in wear and chemical resistance because the $Ca_2ZrSi_4O_{12}$ crystals positively affected physical and mechanical properties.

Keywords: $CaSiO_3$; $Ca_2ZrSi_4O_{12}$; Glass-ceramics; Glazes; Wear resistance

1. Introduction

Recently, research on ceramic tiles has been concerned with crystallized glazes, as glass-ceramics, because of the need for floor and wall tiles to be usable in severe conditions such as wear by wind and chemical attack.[1–3] To satisfy the requirements of glass–ceramic glaze, which are chemical inertness, smoothness, resistance to abrasion and scratching and good mechanical strength, glazes should be carefully designed by microstructural modification with a proper devitrification process. Crystallized glazes would be produced by control of the factors of basic composition, nucleating agents, and heat treatment to determine crystal phases, size and crystallinity.

For tile glaze, the $CaO–ZrO_2–SiO_2$ (CZS) glass system has been studied for several years at Modena University and has shown good properties as a new glaze for tiles using either microwave or conventional heating sources.[2–5] However, their research area is limited to a narrow range of compositions, 55% SiO_2–33% CaO–12% ZrO_2; 52% SiO_2–32% CaO–16% ZrO_2; 51% SiO_2–31% CaO–11% ZrO_2–6% $Li(Na, K)_2O$ (in wt.%) and the effect of each component on the formation of glaze has not been investigated.[4,5] The range of composition in the system is supposed to be designed based on the tentative CZS melting phase diagram, which was published earlier in 1954.[6] As a matter of fact, they reported the application of the CZS system on the basis of a composition belonging to the ternary phase diagram in the stability field of wollastonite for useful and suitable coating for clay products. In fact, ternary phases from the system, $Ca_2ZrSi_4O_{12}$, $Ca_3ZrSi_2O_9$, and $CaZrSi_2O_9$, missing in Ref. [6], were reported later.[7,8] Considering the published information on the glass system, the compositions chosen[3–5] which lie in wollastonite and other phase together, do not suggest any clear reason on the phase stability after cooling from molten glass. When other minerals like wollastonite ($CaSiO_3$), zircon (ZrO_2SiO_2) and quartz (SiO_2) are considered for use as raw materials, conditions for glaze formation should be clarified in terms of required composition to form glasses for frit. In addition, properties of glazes based on CZS glass system that are important for application to tiles have not been reported except hardness and microstructure information on the effect of ZrO_2 content (12 and 15 wt.%).[4,5]

In this work, widely varying compositions, physical and mechanical properties including thermal and wear

* Corresponding author.
E-mail address: hskim@sunchon.ac.kr (H.S. Kim).

0955-2219/03/$ - see front matter © 2003 Elsevier Ltd. All rights reserved.
doi:10.1016/S0955-2219(03)00089-X

properties were studied in order to provide general information needed to find a proper, optimum condition for glazes and to apply the CZS system to other purposes.

Table 1
Chemical composition of raw materials (in wt.%)

Samples	SiO_2	CaO	ZrO_2
C	54	33	13
D	53	33	14
G	55	31	14
H	55	30	15
I	51	37	12
J	53	35	12
K	57	31	12
L	59	29	12
M	56	34	10
IB	51	34	15

2. Experimental procedure

The glass compositions (51–59% SiO_2, 29–38% CaO, 8–15% ZrO_2 (in wt.%) using reagent-grade (Fisher Scientific, USA) were melted in Pt-Rh20 crucibles at 1500 °C for 3 h and the melts were quenched in water to obtain frits (Table 1). The frits were wet-milled to a powder (< 38 μm) using water as a media solution. The glass transition and the crystallization temperatures were determined with a differential thermal analyzer (DTA, TA instrument 1500, USA) on samples ground to a grain size of less than 38 μm, coarse powders (38–106 μm (for C sample), 150–300 μm) and bulk samples (to remove particle size effect, about 30 mg glass powder was melted in a DTA crucible and the crucible was removed from the furnace and cooled to room temperature). Glazing was done on a ceramic tile after preparing a slurry with 79.995% of distilled water, 0.005% binder (CMC, Sodium Carboxymethyl Cellulose, Aldrich), and

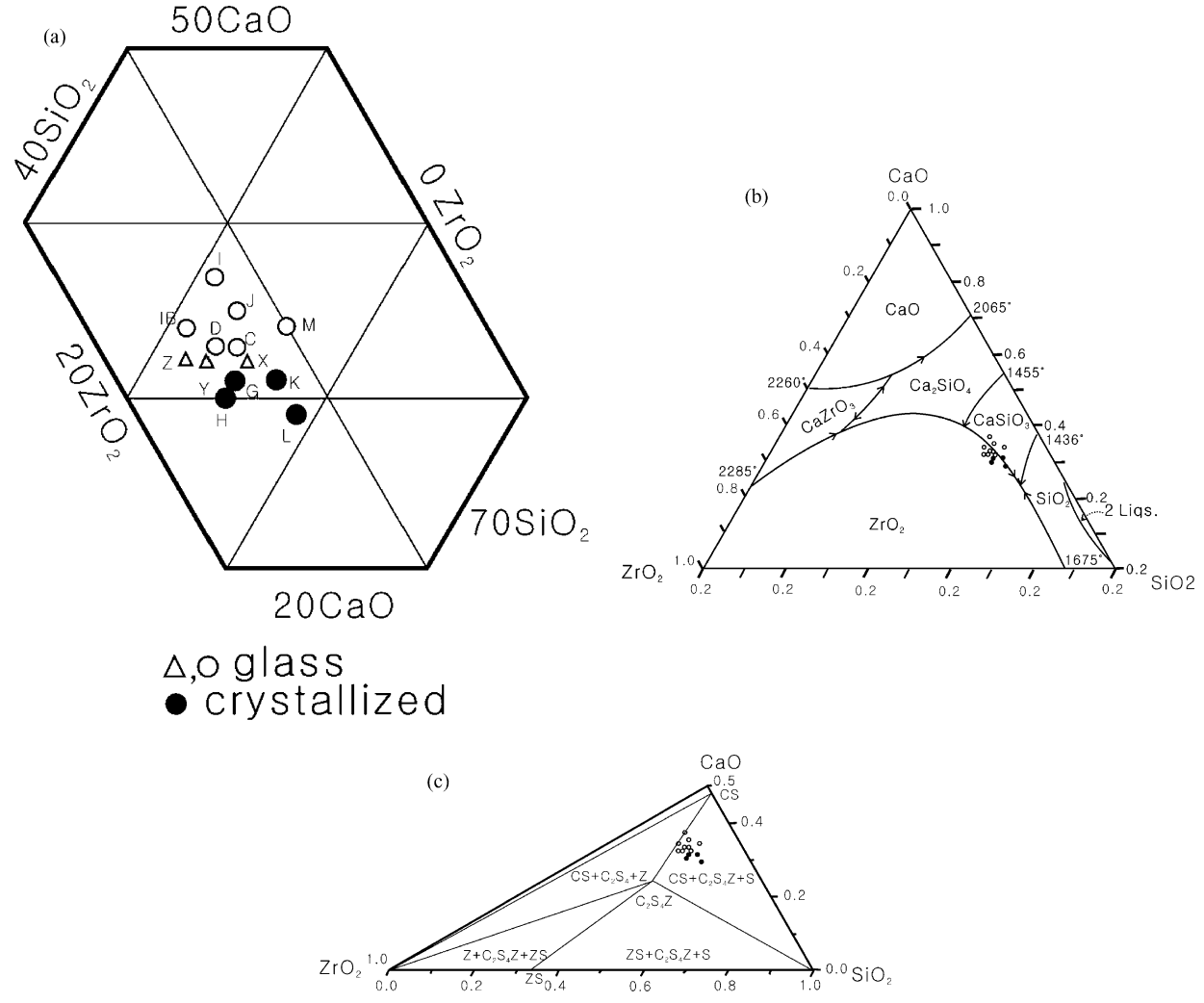

Fig. 1. (a) Glass forming region in the CaO–ZrO_2–SiO_2 system (wt.%) where compositions of X, Y and Z are from Refs. [4 and 5]. (b) Phase diagram of the CaO–ZrO_2–SiO_2 system published by Matsumoto et al. (in 1954),[6] with the compositions of the glasses investigated. (c) Isothermal phase diagram of the CaO–ZrO_2–SiO_2 system at 1400–1500 °C,[8] with the compositions of the glasses investigated.

20% of glass powder (in vol.%). In addition, glass powders were pressed at 5 MPa to form pellets which were sintered at 1000–1200 °C for 10–60 min for the evaluation of physical and mechanic al properties.

Samples were analyzed with an X-ray diffractometer (XRD, Rigaku, Japan, Cu target, scan speed: 2°/min) for the identification of crystal phases. Density and open porosity of sintered samples were measured by Archimedes method. The hardness of samples was tested using a Vickers hardness tester (ASKASI Co. Japan) under 4.9 N for 15 s. Erosion testing was carried out by a dropping SiC powder (size;1.70 mm) test and impacting on the samples at an angle of 45 (KS L1001: Ceramic tiles, 2001). The powder feed rate and average velocity were 1250 g/min and 4.64 m/s, respectively. The reduced weight of samples was quantified as eroded weight per unit area (g/cm^2). For the chemical stability of glaze, samples were inserted in a 6 N HCl solution for 6 h and the reduced weight of each sample was determined as the weight loss per unit volume of samples (g/cm^3). Scanning electron microscopy (SEM, HITACHI, Japan) was used to analyze the microstructure of samples after etching with 4% HF solution for 10 s and HCl for 3 s again. Samples were heated in a dilatometer (Dilatormic, Theta Industrial. Inc., USA) at a rate of 5 K/min up to 950 °C in order to determine thermal expansion coefficients.

3. Results and discussion

3.1. Microstructure

In Fig. 1a, the glass forming result on each composition is represented. During the cooling process in water, the melts of H, K, G, and L were crystallized while the

Table 2
The phases calculated in the $CaSiO_3$–SiO_2–$Ca_2ZrSi_4O_{12}$ compatible triangle

Compositions	Phases (%) (calculated from Fig. 1c)			Phases (found from experimental)		
	SiO_2	$CaSiO_3$	$Ca_2ZrSi_4O_{12}$	SiO_2	$CaSiO_3$	$Ca_2ZrSi_4O_{12}$
M	8	40	52	O	O	O
C	5	49	46	–	O	O
Z[a]	7	50	43	–	O	O
IB	–	43	57	O	O	O

[a] Composition: Z; 52 SiO_2–32CaO–16ZrO_2 (wt.%).[4]

Table 3
Crystalline phases of glass–ceramic heat treated at 950–1100 °C

Compositions	Heat treatment condition [temperature (°C)–time (min)]	$CaSiO_3$	$Ca_2ZrSi_4O_{12}$	SiO_2	Glass
M	950–30	0		00[a]	0 40%[b]
	1000–10	0	0	0	
	1010–30	0	0		
	1050–10	0	0	0	
C	1010–30	0	0	0	
	1050–10	0	0	0	
IB	950–30	0		00	0 28%
	1000–10	0		0	
	1010–5				0
	1010–10	0	0	0	0
	1010–30	0	0	0	0
	1010–60	0		0	0
J	1000–30	0	0		
	1050–30	0	0		
	1100–30	0	0		

[a] 00 means relatively strong peak.
[b] Crystallinity.

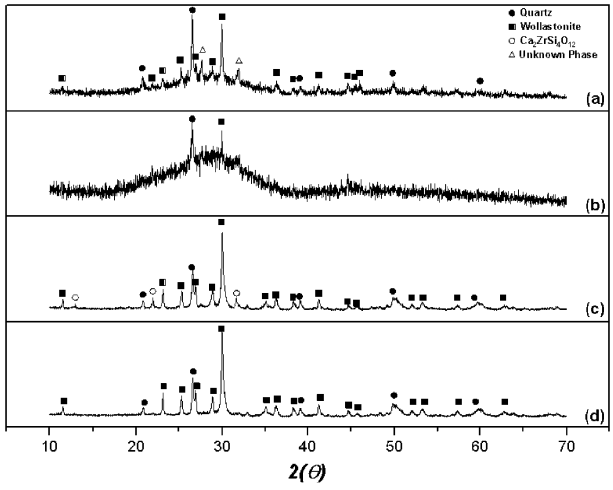

Fig. 2. XRD patterns of glass–ceramics (a) M and (b) IB heat treated at 950 °C for 30 min, (c) M and (d) IB heat treated at 1000 °C for 10 min.

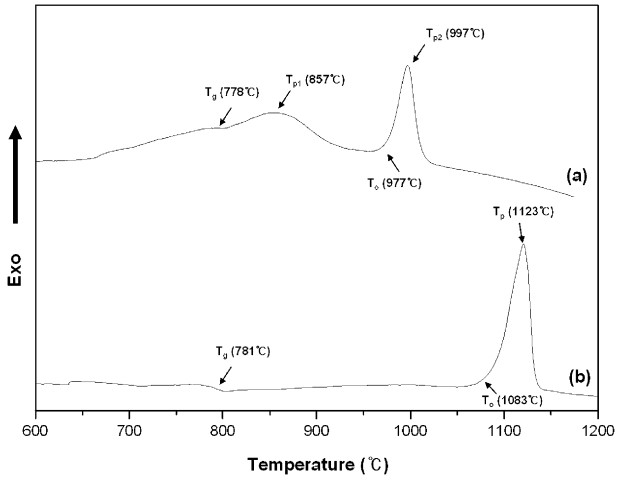

Fig. 3. DTA curves for the C glass: (a) fine powder (<38 μm) and (b) bulk glass at 10 °C/min).

others were glassy. The glass composition of less than 31 wt.% of CaO and more than about 10 wt.% of ZrO_2 resulted in crystallized glasses at room temperature during quenching.

The compositions studied are marked on a phase diagram of CZS [Fig. 1(b)] and a partial isothermal section at 1400–1500 °C [Fig. 1(c)]. The phase diagram (CZS) made by Matsumoto et al.[6] is not correct when the current and other results[7,8] are considered. As a primary phase, zircornia (ZrO_2) appears and later $CaSiO_3$ and SiO_2 comprise the compositions from Fig. 1b. However, the isothermal sections at 1400–1500 °C[8] [Fig. 1(c)] and appearance of $Ca_2ZrSi_4O_{12}$ phase from our work suggest that a four phase eutectic reaction involves an invariant point which lies within the compatibility triangle of the $CaSiO_3$–SiO_2–$Ca_2ZrSi_4O_{12}$ solid phases.

Regarding the composition of glasses, there are two groups in Fig. 1(c), which lie on the boundary ($CaSiO_3$–$Ca_2ZrSi_4O_{12}$) and within a compatibility triangle ($CaSiO_3$–SiO_2–$Ca_2ZrSi_4O_{12}$) based on the crystal formations at 1400 °C.[7,8] Upon cooling, I, and IB glasses would contain $CaSiO_3$ and $Ca_2Si_4ZrO_{12}$, while C, D and others have $CaSiO_3$,$Ca_2Si_4ZrO_{12}$ and SiO_2, crystalline phases [Figs. 1(c) and 2]. In these experiments, the crystal phases of sintered material (M, IB) at 1000 °C are $CaSiO_3$ (JCPDS No.27-0088), $Ca_2ZrSi_4O_{12}$ (JCPDS No.49-0696), and SiO_2 (46-1045) (Fig. 2). In spite of the

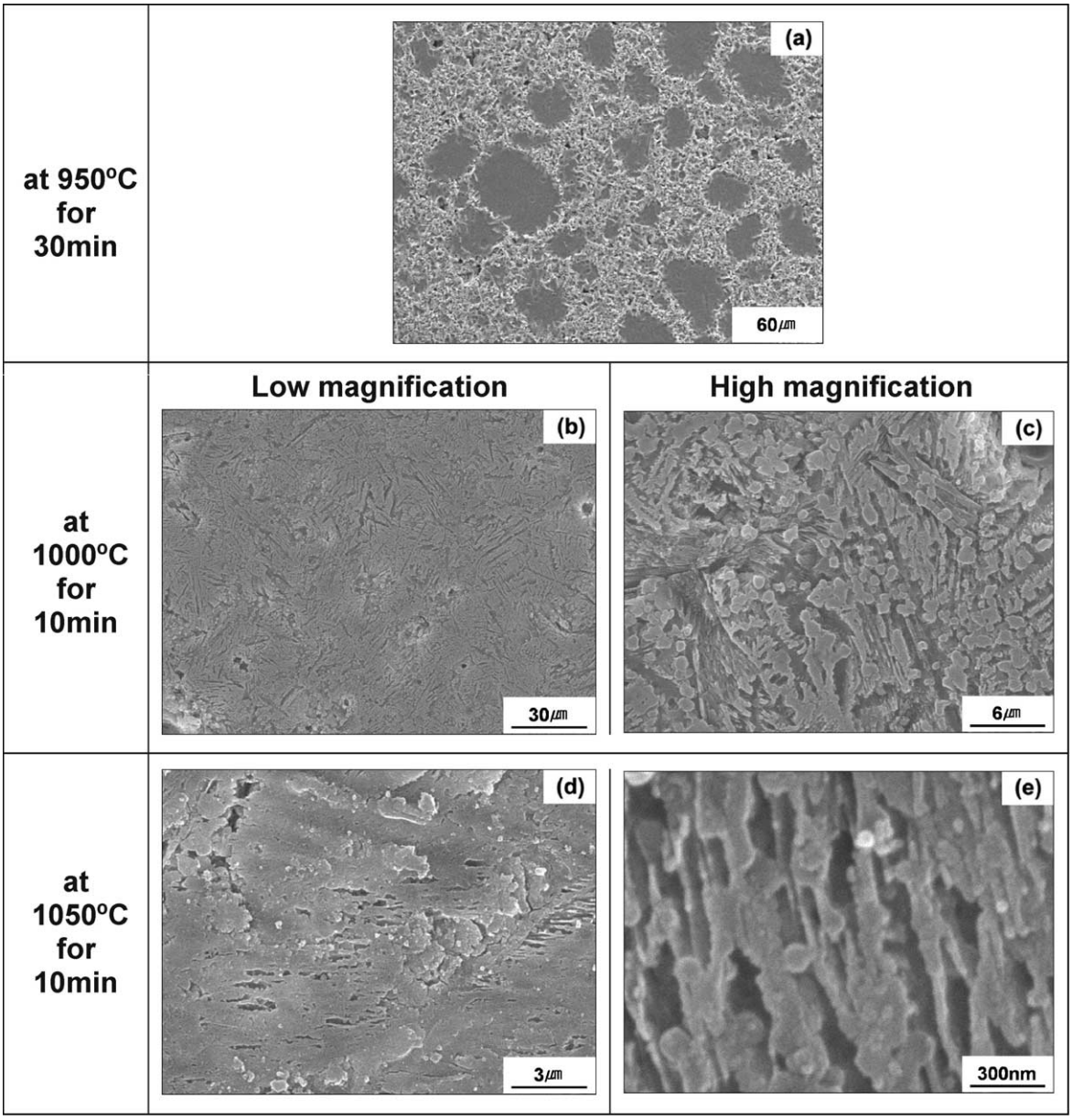

Fig. 4. SEM images after etching showing surface crystals (a), surface and internals (b, c) in glass–ceramics (M) heated to (a) 950 °C for 30 min, (b) 1000 °C for 10 min, (c) detail of sample (b) under high magnification, (d) 1050 °C for 10 min, and (e) detail of sample (d) under high magnification.

absence of SiO_2 in IB based on Fig. 1c, the glass–ceramic (IB glass) heat treated at 950–1000 °C showed a very strong peak of SiO_2 in the XRD patterns (Fig. 2, Table 2). This could be attributed to a different temperature isothermal section, however the same effect is seen for J (Table 2), suggesting that the area of compatibility triangle ($CaSiO_3$–SiO_2–$Ca_2ZrSi_4O_{12}$) depends on temperature. With increasing temperature, the second phase in all compositions, $Ca_2ZrSi_4O_{12}$ increased and SiO_2 decreased (Table 3). On the other hand, the unknown phase found at 950 °C in Fig. 2(a) and (b) disappeared at 1000 °C [Fig. 2(c) and (d)] and it played nuclei to form $Ca_2ZrSi_4O_{12}$. Thus, $Ca_2ZrSi_4O_{12}$ appears at high temperature and long heat treatment time. It was not found that ZrO_2 content affects the formation of crystalline phase from IB, C and M compositions (Table 2). According to an earlier result,[5] however, below 1100 °C, only $CaSiO_3$ appears and above 1150 °C, $CaSiO_3$, $Ca_2ZrSi_4O_{12}$, and ZrO_2 form from the composition of X, Y and Z, which is not matched to the result of the present study and the analysis of isothermal phase diagram [Fig. 1(c)]. In fact, for M, C, X and IB compositions, the

Table 4
The effect of glass power size on thermal analysis (temperature = °C)

Glasses	Fine powder (−38 μm)					Bulk/coarse powder glass				Bulk/powder
	T_g	T_o	T_{p1}	T_{p2}	T_l	T_g	T_o	T_p	T_l	
C	778	810	856	997	–	781	1083	1123	–	Bulk
D	773	807	846	960	–	774	1097	1149	1270	Bulk
I	781	807	850	947	–	774	1053	1110	1268	Bulk
J	785	804	857	983	–	787	1098	1158	1281	Bulk
IB	813	–	949	1019	1240	802	1052	1087	–	Coarse powder (212–425μm)
M	775	–	959	1004	1230	775	1006	1047	–	Coarse powder (212-425μm)

T_o = the onset of crystallisation temperature.
T_p = the exothermal peak temperature, (T_{p1} = the first peak, T_{p2} = the second peak).
T_l = the liquidus temperature.

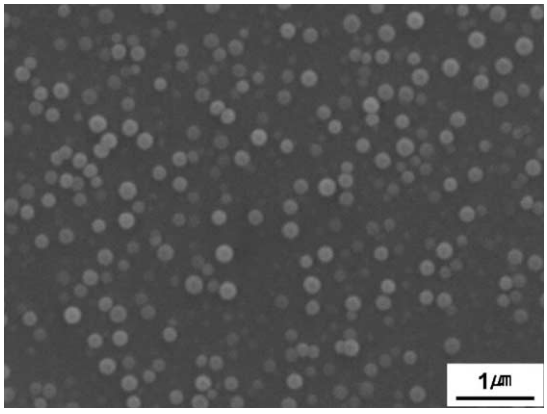

Fig. 6. Interior of the bulk showing nuclei formation in glass-ceramics (M, IB) heated to 950 °C for 20–60 min.

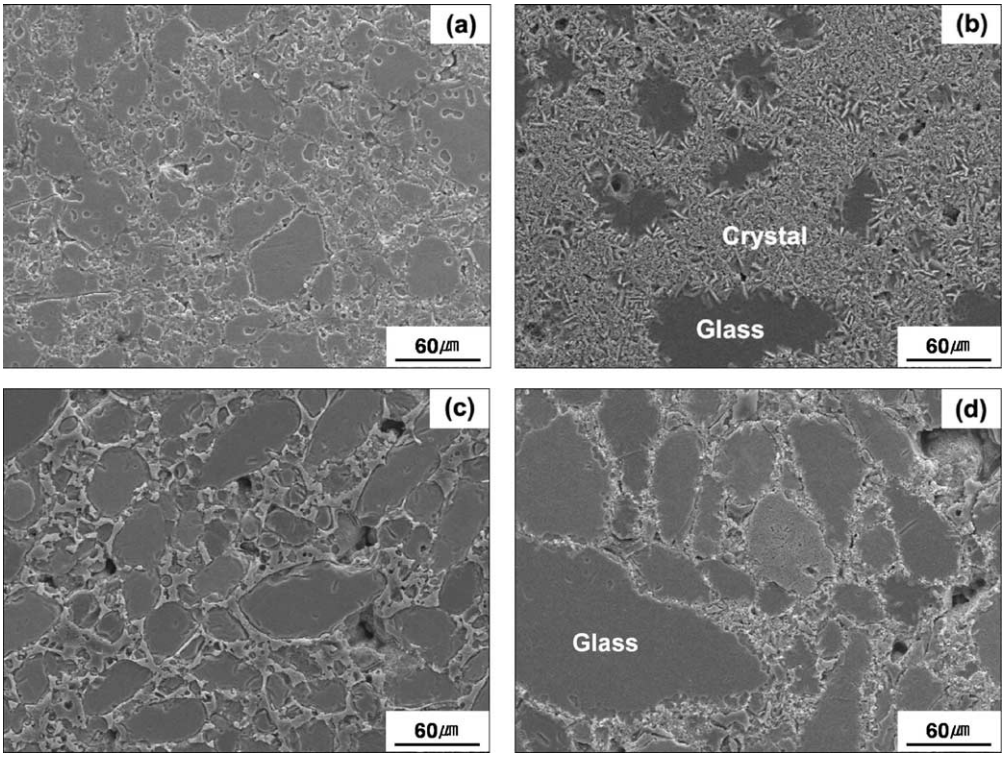

Fig. 5. Etched surface of glass-ceramics (M, IB) showing the formation of surface crystal. Heat treated for (a) 20 min (M) (b) 60 min (M), (c) 20 min (IB), and (d) 60 min (IB) at 950 °C.

relative portion of each phase determined from the phase diagram [Fig. 1(b)] is summarized in Table 3.

The glass transition temperature (T_g), the onset of crystallization temperature (T_o), and the exothermal peak temperature ($T_{p1,2}$) of C glass appeared clearly as represented in Fig. 3. A bulk sample of C glass showed only a single exothermic peak ($T_{p2}=1123$ °C) at high temperature, while a powder sample showed two exothermic peaks containing a peak at a lower temperature. The peak ($T_{p1}=857$ °C) at a lower temperature increased in intensity and shifted towards lower temperature as glass sample size decreased. Therefore, considering the effect of particle size on crystallization, the first peak is related to surface crystallization and the second peak internal crystallization. In Table 4, the result of effect of glass size on thermal analysis (DTA) suggests a combined surface and internal crystallization mechanism in the CZS system.

Fig. 4 shows a sequence change of microstructure with increasing temperature in the range of 950–1050 °C for a short time (10–30 min). At 950 °C, surface crystallization is predominant stage [Fig. 4(a)] and nuclei form in large glass particles as shown in Fig. 5. At 1000 °C, internal crystal grows from nuclei formed at 950 °C [Fig. 4(b) and (c)]. In the microstructure shown in Fig. 4(b) and (c), the fraction of internal crystals is very small compared to surface crystals because of the high surface crystal growth rate. With increasing temperature, the internal crystals grow and show a punch of columnar structure with the formation of micro pores at 1050 °C [Fig. 4(d) and (e)]. As shown in Figs. 5 and 6 for the internal crystals nuclei formed in the middle of glass particle with surface crystallization at 950 °C for 20–60 min. Energy dispersive X-ray analysis (EDX) of

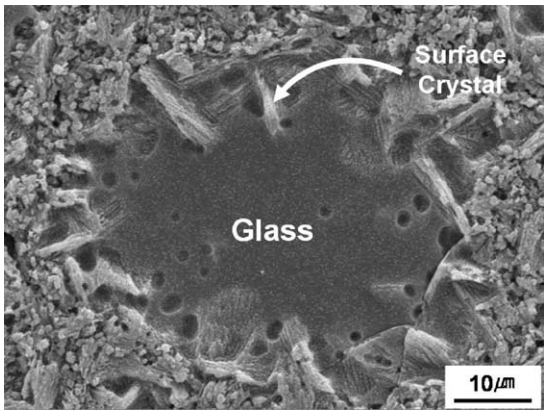

Fig. 8. SEM images after etching showing surface crystals grow in the vicinity of surface: glass–ceramic (M) heated to 950 °C for 60 min.

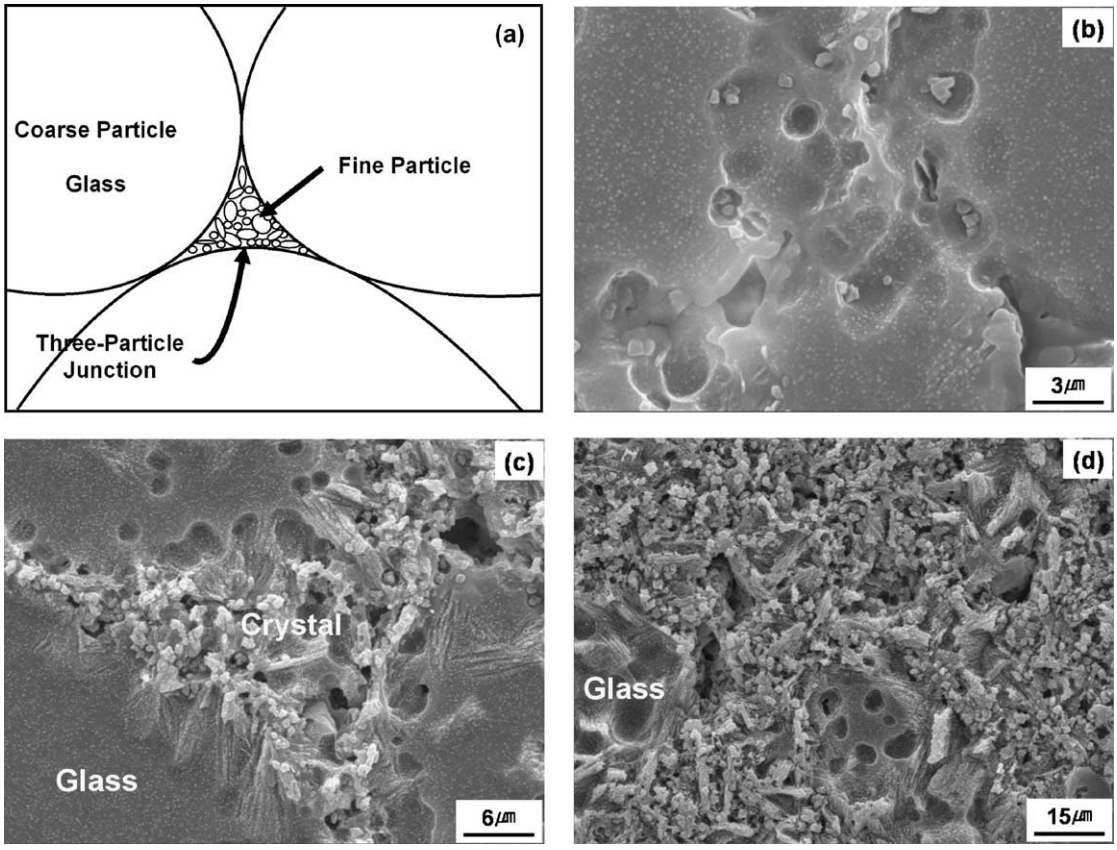

Fig. 7. Sequence of crystallisation at a triple point (or three-particle junctions) (a) of glass powders (M) with increasing time at 950 °C (b) for 20 min, at the beginning stage of the viscous flow; (c) for 30 min, surface crystallisation starts and fine glass powders are fully crystallized; (d) for 60 min, high crystallinity due to fast surface crystal growth rate.

the nuclei in Fig. 6 revealed and the composition, $Ca_{1.2}Si_{4.3}Zr_{0.2}O_8$.

Thus, with the XRD result of sintered samples, it seems that $CaSiO_3$ formed by surface crystallization and $Ca_2ZrSi_4O_{12}$ by internal crystallization [Fig. 4(b) and (c)]. On the other hand, the effect of time on the glass sintering at fixed temperature is very strong as shown in Fig. 7. Fig. 7(b) shows the neck of growth at a triple point (or three-particle junctions) of glass particles due to viscous flow as an early stage of glass sintering without crystallization, but, soon surface crystal appears in Fig. 7(c). Further heating (for 60 min) gives dominant surface crystallization phenomena suggesting small glass particles were completed for crystallization [Fig. 7(d)], while crystals from surface grow toward the center of large ones (Fig. 8).

The microstructure of samples sintered at 1000 and 1050 °C for 30 min showed many pores with 10 μm sizes, which were introduced through the glass sintering process [Fig. 4(b)]. The morphology of pores changed insignificantly from spherical to irregular due to crystallization, as temperature and heating time increased. As shown in Fig. 2, the T_g of D and J are 773 and 785 °C, respectively, and the onset of crystallization temperatures in D and J are 807 and 804 °C, respectively. Therefore, the glass sintering should be completed in that range of temperature to reduce the number of pores as well as to density green samples, but a subsequent crystallization process is required to produce crystals in the glass. In producing crystallized glazes, it is reasonable to sinter and crystallize simultaneously because it is economically important to use only a single stage heat treatment.

3.2. Properties

The apparent density and the open porosity of glaze sintered as a function of temperature and time are given in Fig. 9. The density decreases very gradually with increasing temperature. The decrease of density at high temperature resulted from surface crystallization forming crystals and pores, which reduce sinter ability of the glass powder (Fig. 3). The sintered materials have lower densities compared to the mother glasses (the average

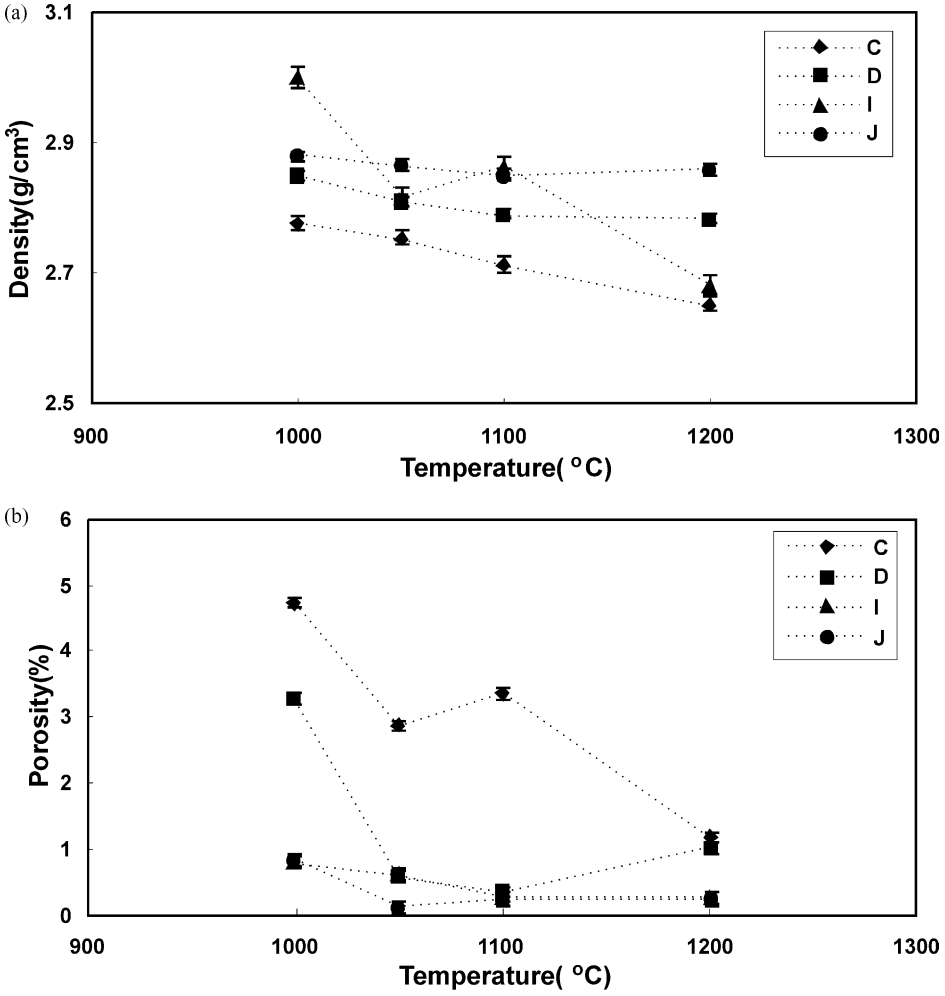

Fig. 9. (a) Bulk density and (b) open porosity of glass–ceramics at different sintering temperatures for 60 min.

density of glasses C, D, I and J is 3.24 g/cm^3) with increasing heat treatment. This is due to the lower theoretical density of $CaSiO_3$ (2.91g/cm^3) and $Ca_2ZrSi_4O_{12}$ (3.112 g/cm^3),[9] and the increased volume of pores formed at high temperature even though the effect of pores on the microstructure is minor. As shown in Fig. 9(b), the porosity of D, I and J sinters are similar to each other and decreased as sintering temperature increases. Similar phenomena were observed in the microstructure as shown in Fig. 4. However, above 1100 °C the porosity increased and, above that temperature, high crystallinity reduced the proportion of residual glass and increased the number of pores (Fig. 4). C sample showed higher porosity at all temperatures because, compared to others, the composition has a high content of SiO_2, which induce high viscosity as confirmed by thermal analysis, which showed high T_g and T_p in Table 4.

The Vickers hardness of sinters shown in Fig. 10(a) and (b) decreases gradually with increasing sintering temperature, but it showed a slight increase with increasing holding time after 30 min. The Vickers hardness was found to be about 6 GPa for samples heat treated at above 1000 °C and for more than 10 min holding time. J composition shows a slightly higher hardness compared to others. However, if samples were heat treated at a higher temperature and for a longer time, the hardness of the glaze decreased as shown in Fig. 10(a). This seems to result from the change of microstructure during crystallization. The C composition had the lowest hardness, which is related to the high porosity as shown in Fig. 9(b). In the early stage of sintering, the hardness of IB increases faster than M and quickly increase to a saturated hardness. The trend of Vickers hardness with increasing time, as shown in Fig. 9(b), is closed to the crystallinity of sintered glass-ceramic for IB sample (Fig. 11).

The erosion rate of glazes is represented in Table 5, in which D and J glazes showed good wear resistance. Proper heat-treatment time resulted in a good erosion rate: at 1050 °C for 30 min, rather than for 10 or 60 min at the same temperature. The increasing hardness of the glaze corresponds to the decreasing erosion rate, as shown by the J composition having high hardness and good wear resistance.[10] The reason is that tiny crystals

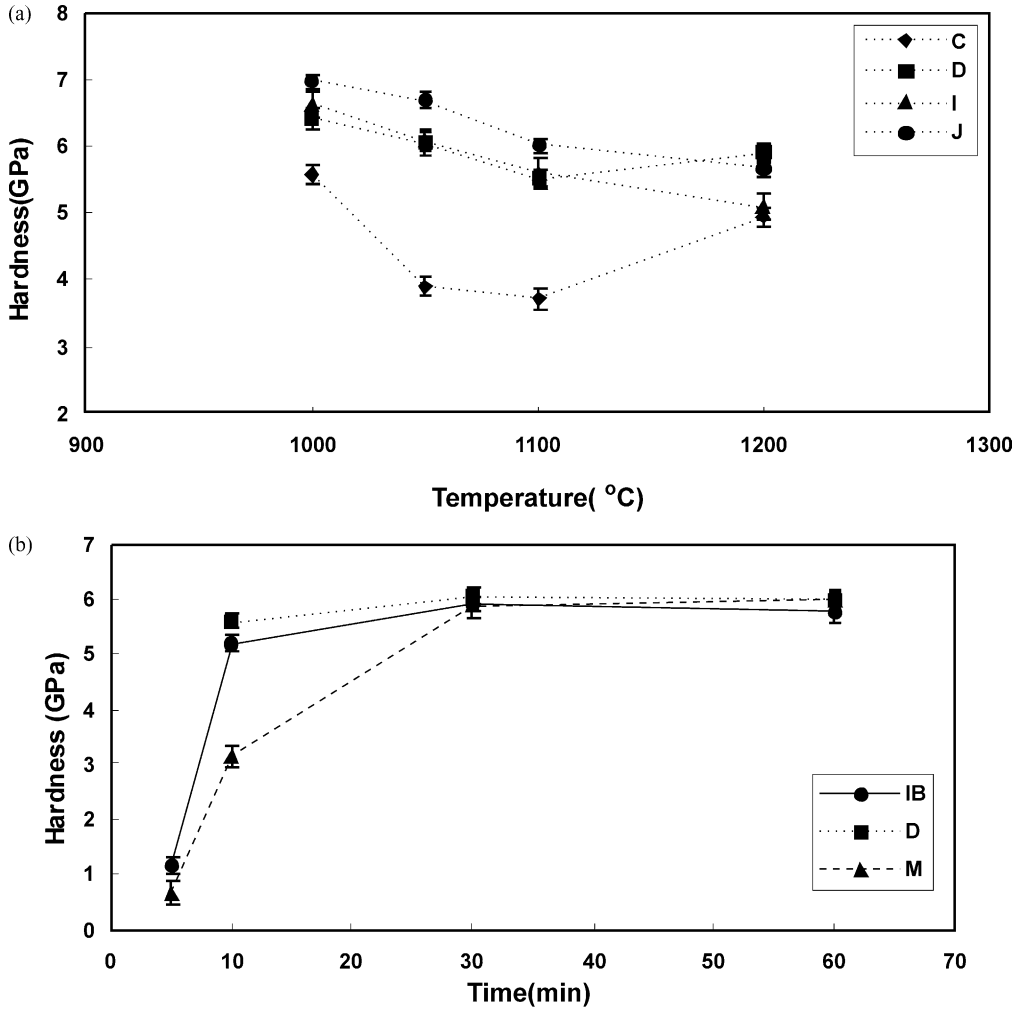

Fig. 10. Vickers hardness of glass–ceramics (a) at different sintering temperatures for 60 min (b) for different sintering time at 1050 °C.

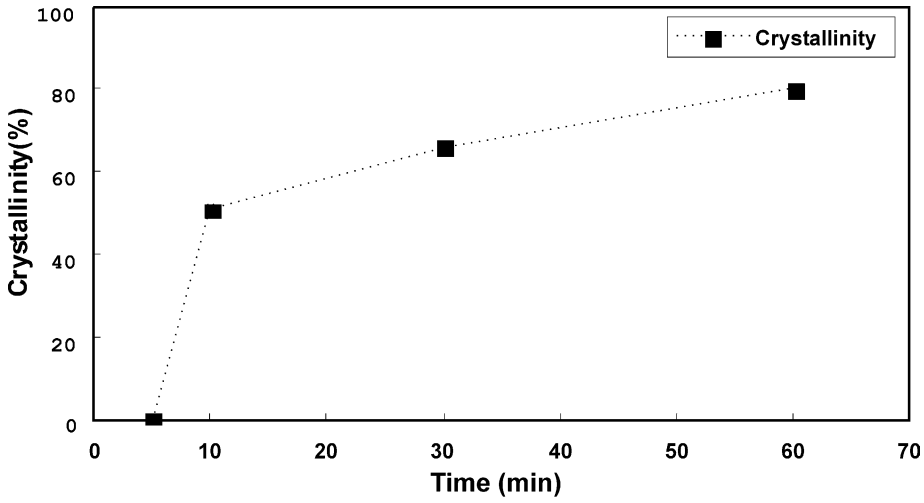

Fig. 11. Crystallinity of glass–ceramic (IB) as a function of sintering time at 1050 °C.

Table 5
Wear rate and chemical durability of glazes sintered at 1050 °C for 30 min

Properties	C	D	I	J
Erosion test, wear rate ($\times 10^{-4}$ g/cm^2)	9	2	4	3
Chemical durability, weight loss ($\times 10^{-1}$ g/cm^3)	0.4	1.6	1.2	10

formed in the glass after firing (sintering) control the physical and mechanical properties of glaze. In terms of the effect of composition on the wear rate of the glaze, it is known that ZrO_2 improves the elastic constant of residual glass and increases wear resistance. 4–10 wt.% of ZrO_2 is effective for the mechanical properties, but higher content is not recommended because it induces devitrification of the glass during the preparation of the frit.[11] However, the current study increased the content of ZrO_2 to 14 wt.% to produce frit containing ZrO_2. Thus, the maximum range of ZrO_2 seems to be dependent on the composition of the system.

To investigate acid resistance, samples were compared in HCl solution. In Table 5, D and J showed excellent chemical resistance. Both the composition and surface characteristics of glasses are important factors to control the chemical resistance of glass. In general, the resistance depends on the content of SiO_2, which increases acid resistance. The effect of ZrO_2 on acid resistance of glasses is much stronger than CaO in glass science.[12] The chemical reaction rate is directly related to surface area of glasses so that higher porosity samples have poorer chemical acid resistance. The effect of porosity was not noticeable in this work but the content of ZrO_2 in CaO–ZrO_2–SiO_2 system seems to be a strong factor as shown in Table 5.

For D and I compositions, the results of thermal expansion testing are given in Fig. 12, which shows a sudden shrinkage around at 840 °C. If the thermal expansion of the glaze is greater than that of the tile body, it causes cracking phenomena, or, in the opposite

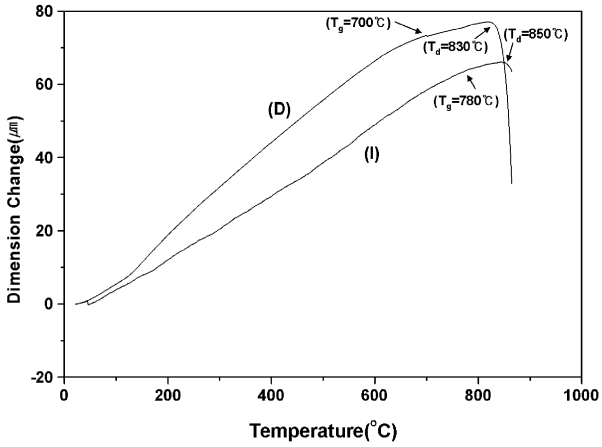

Fig. 12. Thermal expansion of glass–ceramics (D, I).

case, peeling occurs. For a good glaze without any cracks and peeling, the difference of thermal expansion coefficient should be less than 1×10^{-6}/K. In this work, in terms of thermal effect, glazing using the new I and D glazes (which have coefficients of 6.3 and 7.2 ($\times10^{-6}$/K), respectively) on a ceramic tile body (7.3×10^{-6}/K) was done and the resulting samples had no included defects such as cracks in the glaze at all.

4. Conclusion

A sintering process using an electrical resistance furnace was applied to the CaO–ZrO_2–SiO_2 glass system and the crystallization process was investigated. Microstructures of sinters revealed a typical crystallization of glass: with increasing temperature, surface crystallization occurred in the glass and later a second internal crystallization followed on the surface of glass powder. The results of this study indicates that the physical and mechanical properties of CaO–ZrO_2–SiO_2 glass–ceramic have proven to be satisfactory for tile glazes.

References

1. Eppler, R. A., *Glazes and Enamels, Glass Science and Technology, Vol. 1*. Academic Press, New York, 1983, p. 301.
2. Barbieri, L., Leonelli, C. and Manfredini, T., Technical and product requirements for fast firing glass-ceramic glazes. *Ceram. Eng. Sci. Proc.*, 1996, **17**, 11–22.
3. Siligardi, C., D'Arrigo, M. C. and Leonelli, C., Sintering criteria for glass-ceramic frits belonging to the $CaO–ZrO_2–SiO_2$ system. *Am. Ceram. Soc. Bull.*, 2000, **79**, 88–92.
4. Siligardi, C., Leonelli, C., Bondioli, F., Corradi, A. and Pellacani, G. C., Densification of glass powders belonging to the $CaO–ZrO_2–SiO_2$ system by microwave heating. *J. Eur. Ceram. Soc.*, 2000, **20**, 177–183.
5. Siligardi, C., D'Arrigo, M. C., Leonelli, C. and Pellacani, G. C., Bulk crystallization of glass belonging to the calcia-zirconia-silica by microwave energy. *J. Am. Ceram. Soc.*, 2000, **83**, 1001–1003.
6. Matsumoto, K., Sawamoto, T. and Koide, S., Fig. 664. In *Phase Diagram for Ceramists*, ed. M. K. Reser. Am. Ceram. Soc., 1964, p. 231.
7. Kordyuk, R. A. and Gulko, N. V., Fig. Zr-288. In *Phase Diagram for Zirconium and Zirconia Systems*, ed. H. M. Ondisk and H. F. McMurdie. Am. Ceram Soc., 1998, p. 199.
8. Uetsuki, T., Tanaka, K., Maekawa, M., Obata, T., Tamaki, N. and Nakazawa, Y., The compatibility relationships in the system $ZrO_2–CaO–SiO_2$ at 1400–1500 °C. *Yogyo Kyokaishi* (in Japanese), 1985, **93**, 418–425.
9. Powder diffraction file, 49-0696, 42-0550, JCPDS-ICDD, USA, 1999.
10. Volf, M. B., *Chemical Approach to Glass*. Elsevier, New York, 1984.
11. Paul, A., *Chemistry of Glasses, 2nd edn*. Chapman and Hall, 1990 p. 210.
12. Strand, Z. *Glass-ceramic materials*. In *Glass Science and Technology*, Vol. 8. Elsevier, New York, 1986, pp. 76–113.